The electronic density of states in liquids: computer simulation versus integral-equation approach

1993 J. Phys.: Condens. Matter 5 6801

(http://iopscience.iop.org/0953-8984/5/37/002)

J. Phys.: Condens. Matter 5 (1993) 6801–6818. Printed in the UK

The electronic density of states in liquids: computer simulation versus integral-equation approach

Christoph F Strnadl and Gerhard Kahl

Institut für Theoretische Physik, Technische Universität Wien, Wiedner Hauptstraße 8–10, 040 Wien, Austria

Received 10 May 1993

Abstract. A recently developed method due to Winn and Logan (and in a similar formulation by Xu and Stratt) allows the determination of the electronic density of states (DOS) of disordered systems by solving a generalized, complex-valued Ornstein–Zernike-type equation. The only input required is the pair distribution function (characterizing the structure of the disordered system) and the transfer matrix element. A closure relation, necessary for the solution has been proposed by the authors: it is derived—assuming some approximations—from an originally exact relation. Up to now this method has only been applied to model systems, where an exact analytical solution of the equations was possible. For this study we have solved the integral equation along with the closure relation numerically. For the pair interaction of the particles we have considered both hard-core and continuous potentials; various transfer-matrix elements have been used. The results for the DOS have been compared to molecular-dynamics results, where the electronic DOS has been determined by direct diagonalization of the tight-binding Hamiltonian: we find the agreement between the numerical results and the simulation data to be good. Differences may be attributed to the approximations made in the derivation of the closure relation.

1. Introduction

If we are faced with the problem of determining the electronic density of states (DOS) of a disordered system (in particular of a liquid), the main problem we have to cope with is to take into account the full structure of the disordered system, expressed, e.g. in terms of the complete set of multi-particle correlation functions. For the solution of this problem, two major approaches have been developed and utilized during recent years (if we restrict ourselves to a simple tight-binding (TB) model): one is based on simulation methods, where the liquid is simulated by a small ensemble of typically several hundreds or a few thousands of particles; the DOS is calculated by diagonalizing the Hamilton matrix. The other possibility is the determination of the configurationally averaged Green function; although several methods have been proposed for this approach in the past years, it was only a few years ago that a successful concept opened a wider aspect for treating this problem. This approach was proposed by Winn and Logan (WL) [1,2]; a similar formalism has been developed by Xu and Stratt [3].

Winn and Logan considered the following problem: assuming a simple single-band TB Hamiltonian (including both site-diagonal and off-diagonal disorder) how can the ensemble-averaged diagonal and off-diagonal Green functions be determined, taking into account the *full* structure of the liquid in terms of the complete set of s-particle distribution functions $g_s(r_1, \ldots, r_s)$. Using parallels to the determination of the dielectric constant of non-polar

0953-8984/93/376801+18$07.50

fluids based on the classical Yvon–Kirkwood equations—a problem which was solved by Wertheim some time ago [4]—they arrived at a complex-valued integral equation; this equation has formally the same structure as the Ornstein–Zernike (OZ) equation [5] for the determination of the pair-structure of classical liquids. As in the liquid-state case, an additional relation between the unknown functions (a so-called closure relation) is required for its solution: at this point WL are obliged to take recourse to approximations arriving at relations which allow the realization of a numerical solution of the problem. One of their approximations consists in the restriction to a single-site description in which all s-particle correlation functions are approximated by the Kirkwood superposition approximation [6] for $s \geqslant 3$. WL finally arrive at an expression which they call the single super-chain approximation (SSCA), which was also originally suggested by Wertheim for his problem and turned out to be equivalent to the effective medium approximation (EMA) proposed by Roth [7]. Furthermore, WL have succeeded in solving this OZ-type equation along with the SSCA/EMA closure for a simple model system (a step function characterizing the structure of the hard-core system and a Yukawa transfer matrix element) analytically; this was realized by recourse to the analytic solution of the mean spherical approximation (MSA) for a hard-sphere Yukawa system of classical liquid-state theory solved by Waisman and co-workers [8]. They derived a further closure-relation, taking into account at least partly multi-hopping processes (a fact which was completely neglected in the SSCA/EMA), and the generalization of their approach to the two-band model [9]. Both one- and two-band models were compared with computer simulation results (which, however, could not be reproduced in our study and hence leave some questions open [10]). Stratt and co-workers [11, 12] were able to propose an equivalent formulation of the method proposed by WL.

The formalism of the WL approach brings a further advantage: introducing approximations either at the level of the OZ-type equation itself or at the level of the closure relations allows a classification of methods proposed so far [7, 13–16] for the determination of the electronic DOS of disordered systems (as shown in [1]); this makes a more systematic overview possible.

In an effort to apply this powerful method to more complex systems than simple model liquids, a numerical procedure has been implemented which enables us to solve this complex-valued integral equation *numerically* (along with the SSCA/EMA closure relation proposed by WL) and to determine in the following the DOS. This implementation is based on a powerful numerical algorithm, originally devised for the solution of the OZ equation of classical liquid-state theory [17]. It now allows us to determine the electronic DOS for *any* liquid system, characterized by a pair structure (via the pair distribution function (PDF) $g(r)$) and an *arbitrary* transfer matrix element (TME) $V(r)$. A previous study [18] on the influence of these two functions on the DOS for the case of hard-core liquids represents the first numerical application of this numerical method.

The aim of this contribution is the following. (i) since the numerical implementation of the WL method may now be applied to *any* system, we can choose the necessary input quantities (i.e. $g(r)$, $V(r)$ and the density ρ) deliberately and study their influence on the DOS, in particular on its shape and the position of the upper band edge (UBE) (as already partially done in a preliminary communication [18]). For the interatomic forces of the atoms we have used both hard-core (hard spheres—HS) and soft potentials, restricting ourselves in the latter case to simple Lennard-Jones (LJ) systems. The $g(r)$ values have been calculated by means of thermodynamically self-consistent liquid-state theories [19] and computer simulations. Concerning the TMEs, we have used several functional forms, among them the Yukawa TME used by WL: variation of the TMEs enables us to check the reliability of the numerical procedure (when reproducing the analytical results by WL). The

influence of a realistic $g(r)$ instead of a step function as used by WL, is also investigated. (ii) In order to check the reliability of the numerical results we have determined the DOS in computer simulations. The motion of the particles has been calculated by means of a standard molecular-dynamics (MD) simulation; different codes for the hard-core [20] and the soft [21] potentials were used. The DOS itself was obtained by diagonalizing the Hamiltonian using eight k points and averaging over 75–100 independent configurations of the liquid system.

Finally, special attention has been paid to the moments $\langle E^n \rangle = \int \mathrm{d}E\, D(E) E^n$, $D(E)$ being the DOS per particle per energy; these contain useful information about the reliability of the method. The moments were calculated up to second order ($n = 2$) since for these quantities exact relations exist in terms of the PDF and the TME only.

Our results may be summarized as follows: concerning the influence of the PDF, the most crucial quantity is the contact value (main peak height) in the hard-core (soft-potential) system. Especially in the hard-core case we find that the use of a realistic PDF (as obtained either from the simulation or a suitable Percus–Yevick (PY) [22–24] or Verlet–Weis [25] parametrization) is absolutely necessary. A model PDF (step function) is not able to reproduce the UBE as compared to 'exact' simulation results: only on using the 'correct' PDF is the UBE shifted into the right position. These results suggest that—physically speaking—the electronic states in the vicinity of the UBE are mainly determined by nearest-neighbour interactions, which strongly confirms the reports of Bush *et al* and Gibbons *et al* [10, 26], who put forward the same argument in the context of very low-density-systems. Although agreement between computer simulation and numerical results is found to be in general satisfactory, differences may still be observed: however, there is evidence that this closure relation is not suitable in the low density regime where multi-hopping processes are neglected: preliminary results with an improved closure relation that takes these effects—at least partly— into account show that this expression gives better results. In the high density region we find that the quality of the agreement depends on the TME (both functional form and range); this situation is analogous to the liquid-state case: there different closure relations (as, e.g., the hypernetted chain or PY approximations [5]) yield results for the liquid structure of different quality depending on the potential used (the interaction potential in liquid state theory corresponds to the TME in the calculation of the DOS). This points out that differences in the DOS are due to those terms neglected in the derivation of the closure relation.

The paper is organized as follows: in the next section we present a brief overview of the WL method and its numerical implementation as well as the simulation technique; we describe the systems treated in this study, characterized by their PDFs and TMEs. Section 3 contains a discussion of the results and the paper is closed by concluding remarks. An appendix contains implementation details about the integral-equation approach.

2. Theory

2.1. Integral-equation approach

In our study we have followed the formulation of the problem due to WL [1, 2]: for a given configuration of the homogeneous liquid of N particles positioned at r_i, the TB Hamiltonian is given by

$$H = \sum_i \epsilon_i c_i^+ c_i + \sum_{i \neq j} V_{ij} c_i^+ c_j \tag{1}$$

where c_i^+ (c_i) is the creation (annihilation) operator for the one-electron state for site i. $V_{ij} = V(r_i - r_j)$ is the TME which enables the excitation to transfer from site i to site j. Although the problem can easily be formulated for the case of site-diagonal disorder (where the ϵ_i are considered as independent random variables with a probability distribution $P(\epsilon_i)$) we restrict ourselves in this contribution to the case of pure off-diagonal disorder, i.e. $P(\epsilon_i) = \delta(\epsilon_i - \epsilon_0)$; furthermore, we assume—without loss of generality—ϵ_0 to be zero. Hence the Hamiltonian in (1) reduces to

$$H = \sum_{i \neq j} V_{ij} c_i^+ c_j. \tag{2}$$

We are interested in the (ensemble-averaged) DOS $D(E)$, which may be obtained as follows: let $G_{ij}(z)$ be the Green function for a given configuration of the particles, i.e.

$$G_{ij}(z) = \langle 0 | c_i (z - H)^{-1} c_j^+ | 0 \rangle \tag{3}$$

where $|0\rangle$ is the vacuum state. We now define the ensemble-averaged diagonal (off-diagonal) Green function $\bar{G}_{ii}(z)$ ($\bar{G}(r_1 - r_2)$)

$$\bar{G}_{ii}(z) = \langle G_{ii}(z) \rangle \tag{4}$$

$$\bar{G}(r_1 - r_2) = \frac{1}{\rho^2} \left\langle \sum_{i \neq j} G_{ij} \delta(r_i - r_1) \delta(r_j - r_2) \right\rangle \tag{5}$$

where $\langle ... \rangle$ denotes the configurational averaging over a system of N particles which interact via an interaction potential $\Phi_N(r_1, ... r_N)$; ρ is the number density. Once we have determined $\bar{G}_{ii}(z)$, the DOS (per individual particle per energy) may easily be calculated from

$$\bar{G}(E \pm i\eta) = X(E) \mp i\pi D(E) \qquad D(E) = -\frac{1}{\pi} \lim_{\eta \to 0^+} \operatorname{Im} \bar{G}(E + i\eta) \tag{6}$$

where η is a positive infinitesimal.

Using parallels to the determination of the dielectric constant of non-polar fluids based on the classical Yvon–Kirkwood equations solved by Wertheim [4], WL succeeded in presenting a closed set of *exact* equations to determine $\bar{G}(z)$. They arrive at the following coupled integral equations:

$$z\bar{G}(z) = 1 + \rho[\bar{G}(z)]^2 \int d^3 r_2 \, H(r_1 - r_2) V(r_2 - r_1) \tag{7}$$

$$H(r_1 - r_2) = C(r_1 - r_2) + \rho \bar{G}(z) \int d^3 r_3 \, H(r_1 - r_3) C(r_3 - r_2). \tag{8}$$

$C(r_1 - r_2)$ (as well as $\bar{G}(r_1 - r_2)$) may be defined in terms of composite graphs consisting of V_{ij} bonds with additional connectors arising from the s-particle distribution functions $g_s(r_1, \ldots, r_s)$, which characterize the liquid structure. Once equations (7) and (8) are solved, $\bar{G}(r_1 - r_2)$ may be determined from

$$\bar{G}(r_1 - r_2) = \bar{G}(z) H(r_1 - r_2) \bar{G}(z). \tag{9}$$

Equation (8) has a similar structure to the OZ equation [5] of classical liquid-state theory

$$h_2(r_1 - r_2) = c_2(r_1 - r_2) + \rho \int h_2(r_1 - r_3)c_2(r_3 - r_2)\,\mathrm{d}^3 r_3 \tag{10}$$

where $h_2(r) = g_2(r) - 1$ and $c(r)$ are the total and direct correlation functions of the liquid, respectively. As in the liquid case, we have to provide a so-called closure relation, which represents a further relation between these functions and the interatomic pair potential and thus enables the solution of the integral equations.

The WL formulation has furthermore the appealing feature that approaches proposed during recent years for the determination of the DOS may be classified according to approximations introduced at the level of the OZ-type equation and/or the closure relation [7, 13–16].

In our study we have used as the closure relation the SSCA: starting from the exact expression for $C(r_1 - r_2)$ WL confine themselves to a single-site description, which is rigorously defined by the following two criteria: (i) all s-body correlation functions $g_s(r_1, \ldots, r_s)$ are approximated by the Kirkwood superposition approximation [6], and (ii) only single-site graphs are retained in $C(r_1 - r_2)$ [1, 2]. In the remaining expression all graphs with crossing internal $h_2(r)$ bonds are neglected, and finally the authors arrive at the following closure relation:

$$g_2(r)C(r) = g_2(r)V(r) + h_2(r)H(r). \tag{11}$$

This approximation was originally suggested by Wertheim in the dielectric context. Furthermore, the SSCA closure relation, along with the OZ-type equations (7), (8) turns out to be formally equivalent to the EMA proposed by Roth [7]. WL succeeded in mapping the solution of (7) and (8) along with the SSCA closure (11) for a model system (Yukawa TME and step-function PDF) to a standard problem of liquid-state theory: the solution of the MSA for an HS Yukawa system, a problem that may be solved analytically, as demonstrated by Waisman and co-workers [8]. Hence WL are able to give an analytic expression for the DOS for this simple model system.

An obvious generalization along the lines already outlined by Elyutin [13] and Winn and Logan [1, 2] would be the inclusion of multi-hopping graphs in the first term of the right-hand side of (11)

$$g_2(r)C(r) = g_2(r)V(r)/\left\{1 - [\tilde{G}(z)V(r)]^2\right\} + h_2(r)H(r). \tag{12}$$

Although taking into account only the multi-hopping processes between a pair of sites this closure would have the additional pleasing property of reducing to the correct low-density limit $\rho \to 0$.

For this study the OZ-type equation was solved along with the closure relation (11) numerically. The program is a generalization of a powerful implementation [27] of Gillan's [17] algorithm to solve the OZ-equation of classical liquid state theory. Details of the program and numerical parameters are compiled in the appendix.

A further quantity we are interested in is the moments $\langle E^n \rangle$, defined as

$$\langle E^n \rangle = \int_{-\infty}^{\infty} \mathrm{d}E\, D(E)E^n \qquad n \geqslant 0 \tag{13}$$

where the following exact moment conditions hold [11]

$$\langle E^0 \rangle = 1 \qquad \langle E \rangle = 0. \tag{14}$$

For orthogonal atomic orbitals one finds

$$\langle E^2 \rangle = \rho \int d^3r\, g(r) V^2(r). \tag{15}$$

WL [28] assume—but have not proven rigorously—that any DOS calculated by a theory based on the OZ-type equation automatically fulfills the normalization condition $\langle E^0 \rangle = 1$.

2.2. *Simulation*

The simulations were realized with a standard microcanonical molecular-dynamics (MD) code, with the usual periodic boundary conditions and minimum-image convention applied. We used two different codes, optimized for the respective system (HS [20] and LJ [21]). The sample size ranges from $N = 343$ to 864 particles, allowing one to study the influence of the system size on the DOS. Starting from an FCC structure, which is then melted, we finally arrive at a liquid structure (which has been checked by studying the PDF). The simulation runs have been extended over 3×10^5–5×10^5 particle moves (HS case) and over 10^4 time steps Δt (Δt was assumed to be 5×10^{-15} s) in the LJ case. The PDF, which may be used as input in the integral-equation approach, was evaluated after every 50–200 configurations (HS) or after every tenth Δt (LJ) and turned out to be sufficiently smooth to be used in the above expressions.

Problems were encountered for dilute HS systems ($\rho^* = \rho d^3 \leqslant 0.1$ and d being the HS diameter) in MD simulations: using the minimum-image convention unphysical overlaps were observed, resulting in a PDF which is non-zero inside the core. However, it turned out that this unphysical behaviour does not affect the results of the DOS: separate calculations with an HS Monte Carlo code and an MD simulation with an *extended* image convention (i.e. the dynamics of the HS system are determined by taking into account the collisions of all particles within a box nine times the original box size) yield results within numerical accuracy.

As has been already pointed out by Hafner and co-workers [29] and recently by Ganguly and Stratt [30], the finite size of the Brillouin zone and hence the energy dispersion necessitate the calculation of the DOS at more $\boldsymbol{k}$ points than just the Γ point, especially for higher densities $\rho^* \geqslant 0.5$.

Let $V_{jk}(\boldsymbol{k})$ be the discrete Fourier transform of the matrix element $V(r_{jk}) = V(|\boldsymbol{r}_j - \boldsymbol{r}_k|)$, $\boldsymbol{r}_j$ and $\boldsymbol{r}_k$ being the positions of two arbitrary sites of a given configuration,

$$V_{jk}(\boldsymbol{k}) = \sum_{\boldsymbol{a}}{}' \exp(i\boldsymbol{k} \cdot \boldsymbol{a})\, V(|\boldsymbol{r}_j - \boldsymbol{r}_k + \boldsymbol{a}|). \tag{16}$$

The summation in (16) ranges over all—in principle infinite—lattice vectors $\boldsymbol{a}$ of the cubic lattice with the prime restricting the summation to cases with $\boldsymbol{a} \neq 0$ for $j = k$. As we are usually dealing with exponentially damped matrix elements (cf. (18)–(20) below) we take into account only the $26 = 3^3 - 1$ supercells directly adjacent to the central cell, the cells farther away giving only negligeable contributions to the sum in (16), but increasing the computation time considerably.

The DOS is then determined by a direct diagonalization of the resulting matrix $V_{jk}(\boldsymbol{k}), j, k = 1, \ldots, N$, N being the number of particles in the simulation. We have used the following eight $\boldsymbol{k}$ points (L is the length of the simulation supercell):

$$\Gamma : (\pi/L)(0,0,0) \qquad M : (\pi/L)(1,1,0) \qquad X : (\pi/L)(1,0,0) \qquad R : (\pi/L)(1,1,1)$$

and

$$\boldsymbol{k}_i = (\pi/2L)(\pm 1, \pm 1, \pm 1)$$

keeping only one $\boldsymbol{k}$ point for each equivalent pair $\boldsymbol{k}, -\boldsymbol{k}$.

The simulation results are given for a system with $N = 500$ particles and are averaged over 75–100 statistically independent configurations. The averaging has been performed by the usual histogram-binning technique with a bin size of $\Delta E = 0.01 V_0$. Note that—on contrast to the results of Bush *et al* [10]—no subsequent fitting procedure has been applied to the simulation data prior to plotting.

2.3. The systems

2.3.1. Interatomic forces and pair correlation functions. Concerning the atomic structure we have considered two systems: HS and LJ systems. The interaction is assumed to be pairwise additive ($\Phi_N(\boldsymbol{r}_1, \ldots \boldsymbol{r}_N) = \sum_{i \neq j} \Phi(r_{ij})$). The systems are characterized in the HS case by the packing fraction η ($\eta = \frac{\pi}{6}\rho d^3 = \frac{\pi}{6}\rho^*$, d being the HS diameter) and for the LJ case by the energy-parameter ϵ and the length scale σ, so that the potential reads

$$\Phi(r) = 4\epsilon\left[(\sigma/r)^{12} - (\sigma/r)^6\right]. \tag{17}$$

The respective PDFs, which are required as input quantity for the integral-equation approach are determined as follows:

(i) HS case: (a) semianalytic parametrization of the analytical solution of the PY equation [22], which allows an accurate determination of $g(r)$ up to 20 HS diameters [23]; however, as we know that this parametrization differs especially for higher densities, from simulation results, in particular near the contact, we also used (b) the semi-empirical parametrization of computer-simulation results due to Verlet and Weis (VW) [25] of the PDF of an HS system; and (c) the PDF as obtained directly from the simulation, restricted, however, to the range [0, $L/2$], i.e. the function is known only up to half the box length ($L = \sqrt[3]{\pi N/6\eta}$). The influence of the different PDFs will be discussed in section 3.

(ii) LJ case: (a) the PDF was obtained by one of the thermodynamically self-consistent liquid-state integral-equation approaches (HMSA [19], MHNC [31]) which are known to give—within numerical accuracy—results equivalent to simulation data [32, 33]; (b) we also obtain directly from the simulation the PDF (again restricted to the range [0, $L/2$]), which turns out to be in good agreement with the PDF as obtained from (a).

2.3.2. The transfer matrix elements. For the TMEs we used—as in our previous study [18]—the following three expressions:

$$V_{\mathrm{Yuk}}(r) = -\left(V_0/x\right)\exp(-\alpha x) \tag{18}$$

$$V_{\mathrm{ov}}(x) = -V_0\left[1 + \alpha x + \tfrac{1}{3}(\alpha x)^2\right]\exp(-\alpha x) \tag{19}$$

$$V_{\mathrm{1s}}(x) = -V_0(1 + \alpha x)\exp(-\alpha x) \tag{20}$$

where V_{Yuk} is a Yukawa TME, V_{ov} is a TME taken to be proportional to overlaps of hydrogen 1s wave-functions, and V_{1s} is the 1s matrix element (assuming hydrogen 1s eigenfunctions). During all calculations—both integral equation and simulation—we use reduced (dimensionless) units throughout. The length is scaled with the intrinsic scale of the system, $x = r/d$ for the HS systems, and $x = r/\sigma$ (cf. (17)) for the LJ system. The matrix elements and the energy are given in reduced units as $V^*(x) = V(x)/V_0^*$, $V_0^* = V_0/d$ ($V_0^* = V_0/\sigma$) for a Yukawa transfer matrix element V_{Yuk} for an HS (LJ) system and $V_0^* \equiv V_0$ otherwise, and $z = E/V_0^*$, respectively. This leads to a reduced DOS (per particle per reduced energy) of $D^*(z) = V_0^* D(E)$.

3. Results

3.1. Overview of previous results of the integral-equation approach

In this paragraph we want to briefly present the results already given elsewhere [18]. Concerning the influence of $g(r)$ we have found [18] that for hard-core systems the contact value $g(d)$ is the most crucial parameter. Figure 1(a) represents the DOS for a fixed TME, V_{1s}, with $\alpha = 2$, for two different densities $\rho^* = 0.1$ and $\rho^* = 0.5$, where we compare a step-function PDF with a realistic PY $g(r)$. The UBE is clearly seen to move upwards—into the right position, as will be discussed below in section 3.2. To further demonstrate the claim that the electronic states near the UBE are mainly determined by the contact value of the PDF we have calculated the DOS in figure 1(b) for two different PDFs (an HS system in the PY approximation and an HS Yukawa (HSY) system in the mean-spherical approximation, the latter also admitting analytical solution) with the same contact value $g(d)$ but fundamentally different long-range behaviour. The PY $g(r)$ has been computed at a packing fraction of $\eta = 0.2712$ whereas the HSY parameters are given by $K = 1$, $\eta = 0.052\,36$ and $z = 1.5$ (see, e.g., [24] for a recent semi-analytic approach): the resulting DOSs differ only marginally. Hence the model system previously proposed by WL, assuming a step-function for the PDF so that $g(d) = 1$, must give substantially different results from a realistic PDF. The physical origin for the dependence of the UBE on the short-range order may be related to an effective (energy and density dependent) screening of the TME [34].

The influence of the TME is more complex. For simplicity we have used only one PDF (a step function, allowing a direct comparison with the analytical WL results for a Yukawa TME) and have calculated the DOS for the three different TMEs (18)—(20) (i.e., we varied both shape and range via α) and different densities. When going from figure 2(a) to figure 2(b) and, thus, reducing the range of the TME, the UBE is progressively shifted to lower energies and we obtain a substantially narrower band, a behaviour well known in any TB approach. Moreover, from figure 2(b) it can be clearly seen that the low-density limit (this is also equivalent to a very-short-ranged interaction, i.e. large α) of the EMA reduces to a Hubbard semi-elliptical DOS centred around $z = 0$. Increasing the density when switching from figure 2(b) to figure 2(c) the UBE is shifted upwards, while the height of the DOS is affected only marginally.

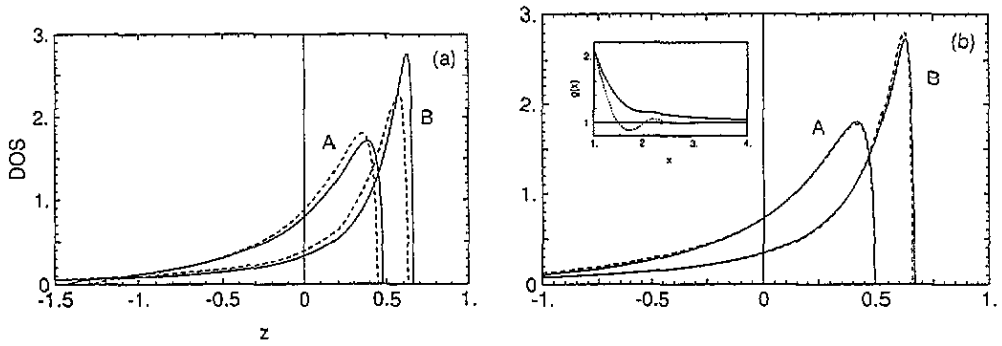

Figure 1. (a) The reduced DOS, $D^*(z)$, for a 1s TME V_{1s} with $\alpha = 2$ for two different PDFs: ——, PY $g(r)$; - - - -, step function. $\rho^* = 0.1$ (curves A) and $\rho^* = 0.5$ (curves B). (b) The reduced DOS, $D^*(z)$, for a V_{1s} TME with $\alpha = 2$ for two PDFs with different long-range behaviour (cf. inset). ——, HS–Yukawa $g(r)$, - - - -, PY $g(r)$. $\rho^* = 0.1$ (curves A) and $\rho^* = 0.5$ (curves B).

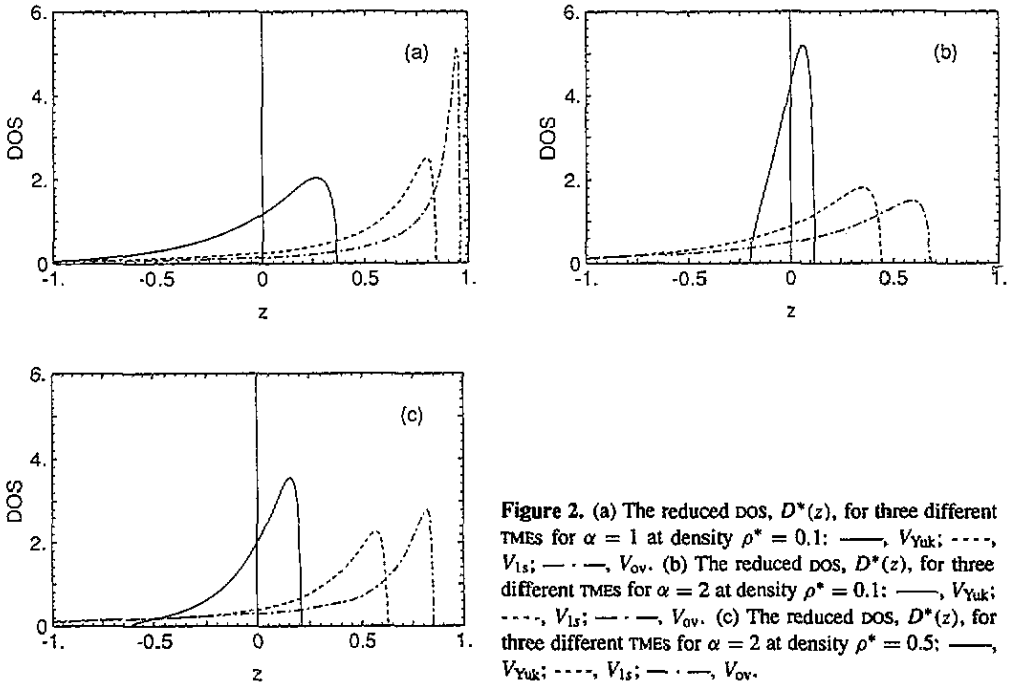

Figure 2. (a) The reduced DOS, $D^*(z)$, for three different TMEs for $\alpha = 1$ at density $\rho^* = 0.1$: ——, V_{Yuk}; - - - -, V_{1s}; — · —, V_{ov}. (b) The reduced DOS, $D^*(z)$, for three different TMEs for $\alpha = 2$ at density $\rho^* = 0.1$: ——, V_{Yuk}; - - - -, V_{1s}; — · —, V_{ov}. (c) The reduced DOS, $D^*(z)$, for three different TMEs for $\alpha = 2$ at density $\rho^* = 0.5$: ——, V_{Yuk}; - - - -, V_{1s}; — · —, V_{ov}.

3.2. Hard-core systems

In our study of HS-systems we have limited ourselves to three particular TMEs (cf. (18)–(20)), for which the DOS has been determined at various densities ρ^* to enable a fairly complete comparison with 'exact' simulation results. We have chosen a $V_{Yuk}(x)$ TME with $\alpha = 1$ (figure 4(a)–4(c)), a $V_{1s}(x)$ TME with $\alpha = 2$ (figure 5(a)–5(c)) and a $V_{ov}(x)$ TME with $\alpha = 2$ (figure 6(a) and 6(b)), with the densities ranging from $\rho^* = 0.1$ to $\rho^* = 0.8$. The PDFs for these systems are displayed in figure 3.

Figures 4–6 are arranged in the following systematic way: when going from (a) to (c)

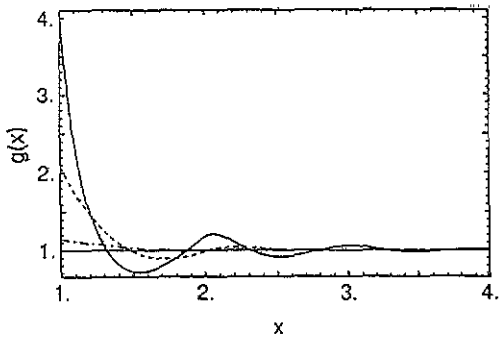

Figure 3. The PY pair distribution functions for an HS system at three different densities.: ——, $\rho^* = 0.8$; - - - -, $\rho^* = 0.5$; — · —, $\rho^* = 0.1$. The $g(r)$ for $\rho^* = 0.8$ is a VW parametrization

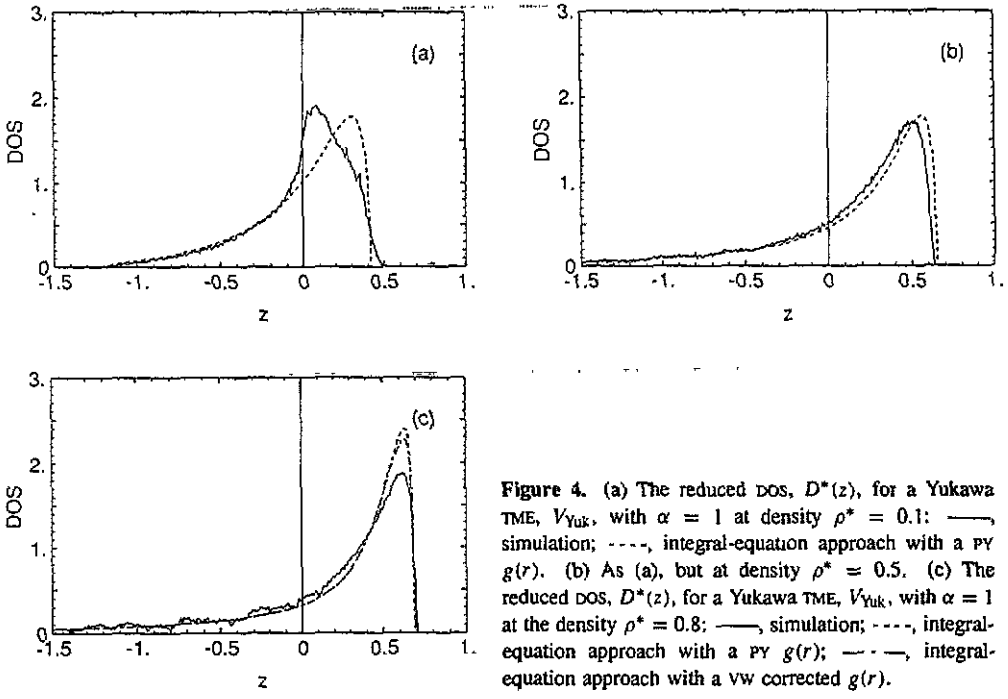

Figure 4. (a) The reduced DOS, $D^*(z)$, for a Yukawa TME, V_{Yuk}, with $\alpha = 1$ at density $\rho^* = 0.1$: ——, simulation; - - - -, integral-equation approach with a PY $g(r)$. (b) As (a), but at density $\rho^* = 0.5$. (c) The reduced DOS, $D^*(z)$, for a Yukawa TME, V_{Yuk}, with $\alpha = 1$ at the density $\rho^* = 0.8$: ——, simulation; - - - -, integral-equation approach with a PY $g(r)$; — · —, integral-equation approach with a VW corrected $g(r)$.

(e.g., from 4(a) to 4(c)), the density is increased gradually while keeping the TME fixed. Switching from one subfigure of 4 to the corresponding subfigures of 5 and 6 (e.g., from 4(b) to 5(b) and 6(b)) the range of the TME is increased at the same fixed density ρ^*. Each particular DOS calculated by the integral-equation approach using the closure relation of (11) is displayed along with the 'exact' DOS as obtained from an HS MD computer simulation, thus enabling a thorough study of the reliability of the SSCA/EMA closure.

In summarizing the outcome of such a comparison we have to distinguish a low-density behaviour and a high-density behaviour of the SSCA/EMA. At $\rho^* = 0.1$ we note that, although the lower band tail is reproduced very well, the upper band and its edge are not determined correctly by the theory. This may well be explained by the fact that the electronic states at the upper band edge are mainly determined by local (pairwise) interactions, as has been

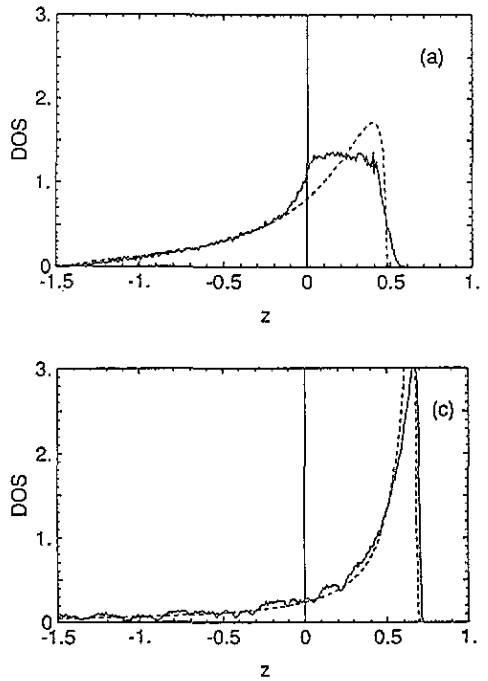

Figure 5. (a) The reduced DOS, $D^*(z)$, for a 1s TME, V_{1s}, with $\alpha = 2$ at density $\rho^* = 0.1$: ——, simulation; - - - -, integral-equation approach with a PY $g(r)$. (b) As in (a), but at density $\rho^* = 0.5$. (c) As in (a), but at density $\rho^* = 0.8$.

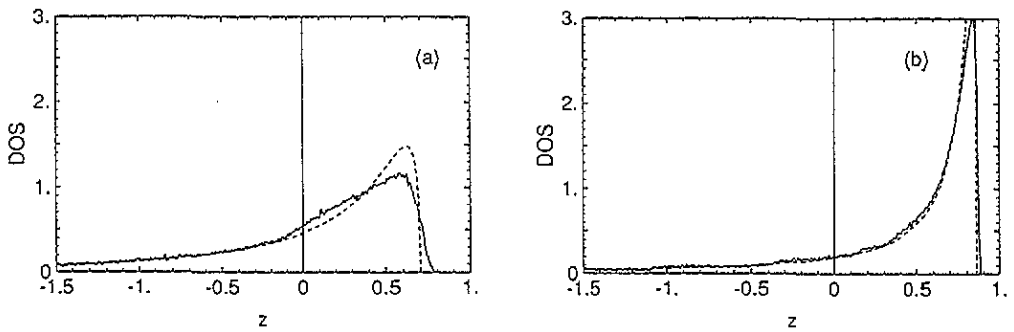

Figure 6. (a) The reduced DOS, $D^*(z)$, for an overlap TME, V_{ov}, with $\alpha = 2$ at density $\rho^* = 0.1$: ——, simulation; - - - -, integral-equation approach with a PY $g(r)$. (b) As (a), but at density $\rho^* = 0.5$.

already put forward in section 3.1. At lower densities $\rho^* \leqslant 0.1$ one would also have to include multi-hopping processes in the expansion of $C(r_1 - r_2)$ to correctly count the contributions of a pair of sites. Those effects are obviously completely ignored in the single-site closure of (11).

The SSCA/EMA results in the high-density regime ($\rho^* \geqslant 0.5$) are much more favourable. Now, both lower and upper tails of the single energy band are reproduced in very good agreement with the simulation data. The UBE and the position of the maximum in the DOS are predicted correctly as are the form and steepness of the flank of the UBE. One notes that this agreement is slightly better for long-ranged TMEs (cf. figures 4(b), 5(b) and 6(b)) than for a Yukawa TME indicating that we still see some multi-hopping influence, as has been

argued in the preceding paragraph.

At these densities, unfortunately, we have to face another deviation of the theory compared to the exact results. Although the position of the maximum in the DOS coincides almost exactly with the simulation, the height as determined from the integral-equation approach is overestimated by a noticeable amount. We will argue that this feature of the SSCA/EMA is due to the selective summation process prescribed by the closure of (11), where even at the single-site level an infinite number of interaction graphs has to be neglected to arrive at an analytical closure relation. This restriction to a certain subclass of all single-site diagrams overestimates, as we will show in a moment, the contributions of the long-range interactions of the electrons in the liquid. In figure 7 we have depicted the DOS for an HS system at $\rho^* = 0.1$ and $\rho^* = 0.5$ for a $V_{\mathrm{Yuk}}(x)$ TME with $\alpha = 1$ along with a 1s matrix element $V_{1s}(x)$ with $\alpha = 2.145$. The range of $V_{1s}(x)$, $\alpha = 2.145$, has been chosen to minimize the differences to the former $V_{\mathrm{Yuk}}(x; \alpha = 1)$ in the range $1 \leqslant x \leqslant 2$, i.e., it has been determined by minimizing the following function of α:

$$\int_1^2 g(x)\,|V_{1s}(x;\alpha) - V_{\mathrm{Yuk}}(x;\alpha = 1)|^2\ \mathrm{d}x.$$

The TMEs determined in this manner will possess a similar short-range behaviour while $V_{1s}(x)$ is much more far-ranged than the corresponding $V_{\mathrm{Yuk}}(x)$. As can be clearly seen from figure 7, at low densities the differences between the two matrix elements are minor, while at $\rho^* = 0.5$ a significant increase of the peak height of the DOS for the long-ranged $V_{1s}(x)$ is to be observed, other deviations being only of marginal influence. This clearly indicates that in the summation process inherent to the closure (11) long-range interactions determine the peak height of the DOS. Switching back to the previous figures 4(c), 5(b) and 5(c), where the same behaviour has been noticed, this would imply that the SSCA/EMA overestimates the contributions stemming from the long-range interactions of the excitations in the liquid system. This fact may be reminiscent of a well known point in simple liquid state theory where different summation prescriptions (viz., closure relations, e.g., HNC or PY [5]) have to be used for long- or short-ranged pair potentials to obtain results in good agreement with exact data. The analogies to the theory of simple liquids may—in our opinion—be stretched even further as we propose to employ some form of 'mixing' between two closures, e.g., (11) and (12), to overcome these difficulties. Of course, a measure for self-consistency would have to be supplied, too, where we would suggest using the moments $\langle E^n \rangle$ of the DOS.

3.3. *Continuous potentials*

When computing the DOS via the integral-equation approach for realistic systems described by continuous interatomic pair potentials we have deliberately chosen the parameters to resemble a well known system: $\epsilon/k_B = 119.80\,\mathrm{K}$, $\sigma = 3.405\,\text{Å}$ (cf. (17)) with the mass of the particles fixed at $m = 6.633 \times 10^{-26}$ kg, which incidentally conforms to liquid Ar. Obviously, any TB approach is not feasible to calculate electronic properties of a real Ar liquid, but we are interested only in the properties of the LJ system itself, not its relation to any real liquid. The DOS has been calculated for two different TMEs, V_{Yuk} and V_{1s}, at two points on the liquidus line, at $T = 90$ K with the number density $n = 0.021\,41\ \text{Å}^{-3}$ and $T = 150$ K, $n = 0.010\,11\ \text{Å}^{-3}$. In order to roughly compare these two systems to an HS system—being fully described by a reduced density ρ^* only—we obtain

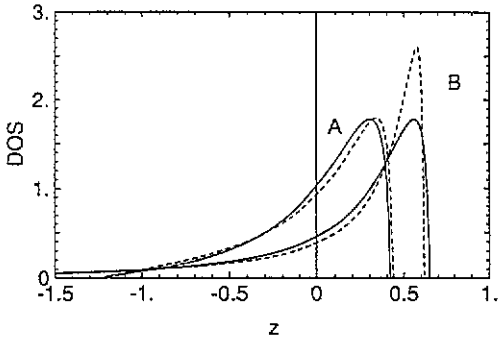

Figure 7. The reduced DOS, $D^*(z)$, for two different TMEs with different long-range behaviour at density $\rho^* = 0.1$ (curves A) and $\rho^* = 0.5$ (curves B) with a PY $g(r)$: ——, V_{Yuk} with $\alpha = 1$; - - - -, V_{1s} with $\alpha = 2.145$.

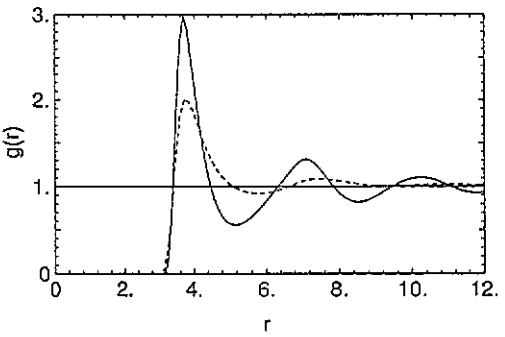

Figure 8. The PDF for the two different states of the LJ system: ——, $T = 90$ K; — · —, $T = 150$ K. For the other parameters characterizing the system cf. text.

$\rho^* = 0.91$ and $\rho^* = 0.41$ respectively; here we have used Barker and Henderson's [36] definition of an equivalent HS diameter d

$$d = \int_0^{r_{min}} d^3r \, \{1 - \exp[-\beta\Phi(r)]\}. \tag{21}$$

For a more detailed description we have depicted the two PDFs in figure 8.

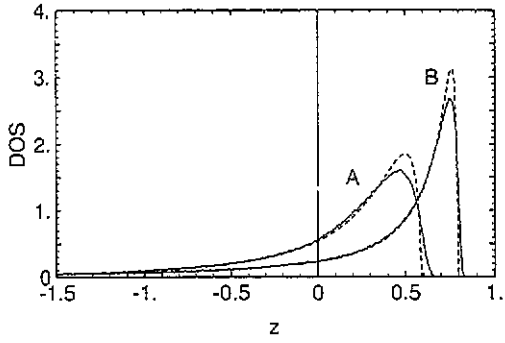

Figure 9. The reduced DOS, $D^*(z)$, for an LJ system at $T = 150$ K for a Yukawa TME, V_{Yuk} with $\alpha = 1$ (curves A) and a 1s TME, V_{1s}, with $\alpha = 1.5$ (curves B): ——, simulation; - - - -, integral-equation approach.

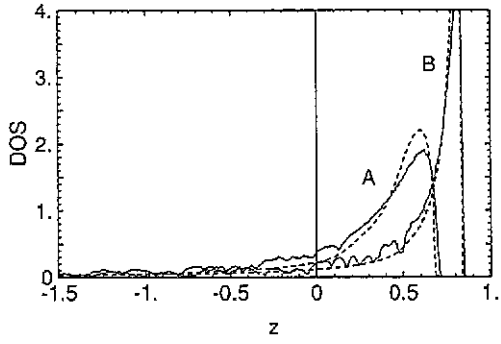

Figure 10. As figure 9, but at temperature $T = 90$ K.

The resulting DOS computed via the solution of the coupled integral equations as compared to 'exact' simulation results are given in figure 9 for the low-density state at $T = 150$ K and in figure 10 for the high-density system at $T = 90$ K. We find the agreement to be reasonably good; especially at $T = 150$ K the band-edge behaviour of both upper and lower band-edges is reproduced in an excellent way. One notes that this fact does not depend on the TME used. As has already been pointed out in section 3.2 one expects

Table 1. The moments $\langle E^n \rangle$, $n = 0$, 1, and 2 of the reduced DOS for the HS systems of this study. The first column, TME, denotes the type of transfer-matrix element used: '1s' for a V_{1s}, 'ov' for a V_{ov} and 'Yuk' for a V_{Yuk} TME.

TME	ρ^*	α	$\langle E^0 \rangle$	$\langle E^1 \rangle$ $\times 10^{-4}$	$\langle E^2 \rangle$ integral equation	$\langle E^2 \rangle$ (15)
1s	0.1	2.0	1.0006	2.54	0.1638	0.1639
1s	0.5	2.0	1.0001	1.96	0.9711	0.9717
ov	0.5	2.0	1.0014	12.38	2.7681	2.7880
Yuk	0.1	0.5	1.0005	14.98	0.5233	0.5292
Yuk	0.1	1.0	1.0007	3.21	0.1096	0.1098
Yuk	0.5	1.0	1.0014	− 1.05	0.6674	0.6717
Yuk[a]	0.8	1.0	1.0003	1.62	1.6906	1.6945
Yuk[b]	0.8	1.0	0.9989	− 7.43	1.2316	1.2741

[a] PY-$g(r)$.
[b] VW corrected PY-$g(r)$.

the EMA to overestimate the maximum of the DOS due to a highly selective summation of graphs prescribed through the closure (11). This effect can be clearly seen in both figures regardless of the TME or the density.

3.4. Moments

Results for the moments are compiled in table 1 for HS systems and in table 2 for LJ systems. The moments provide a convenient tool for measuring the accuracy and stability of the numerical implementation. We find that the exact values for $\langle E^0 \rangle = 1$ and $\langle E^1 \rangle = 0$ are reproduced for all systems within numerical accuracy. The moment $\langle E^2 \rangle$ has been calculated via two routes, either by direct integration of the DOS (13) or by using (15). In general, agreement of both results is better than 99%, only for two cases have larger differences been encountered. This may be attributed to the increased numerical accuracy required for the calculation especially at the far end of the lower band tail. There for some systems the band extends downwards until $z \simeq -12$ and we obviously have a quadratic influence on z (cf. (15)) which multiplies any numerical instability.

Table 2. The moments $\langle E^n \rangle$, $n = 0$, 1, and 2 of the reduced DOS for the LJ systems of this study. The first column, TME, indicates the type of transfer-matrix element used, cf. table 1.

TME	Temperature (K)	α	$\langle E^0 \rangle$	$\langle E^1 \rangle$ $\times 10^{-4}$	$\langle E^2 \rangle$ integral equation	$\langle E^2 \rangle$ (15)
Yuk	150	1.0	1.0013	7.37	0.4812	0.4808
1s	150	1.5	1.0036	28.30	2.2103	2.2084

WL have assumed (but not proven rigorously) that any DOS calculated via an OZ-type equation is automatically normalized (i.e., $\langle E^0 \rangle = 1$), but see also [35], where a different argument based on the relation between the nth moment and the nth term in the locator expansion is put forward. This seems to be confirmed from our data. However, we found from preliminary calculations [37] using a different closure relation, which is a generalization of a theory due to Elyutin [13],

$$g_2(r)C(r) = g_2(r)V(r)/\{1 - [\tilde{G}(z)V(r)]^2\} \tag{22}$$

cases with $\langle E^0 \rangle \neq 1$.

4. Conclusion

In this contribution we have shown the results of a numerical implementation of an algorithm for the determination of the electronic density of states of topologically disordered systems. The theory, originally formulated by Winn and Logan [1,2], is based on the solution of two coupled integral equations with the pair distribution function $g(r)$ characterizing the structure of the liquid medium and the transfer-matrix element $V(r)$ enabling the electronic transfer between different sites. In order to solve these equations an additional equation, the so-called closure relation, has to be supplied. We have taken one particular single-site closure (SSCA/EMA), which effectively renders the theory equivalent to the effective medium approximation of Roth [7].

While previous contributions incorporating the SSCA/EMA approach have only considered analytically solvable model systems (step-function $g(r)$, Yukawa-type transfer-matrix element $V(r)$) [2,3,11], our numerical implementation allows the full solution of the SSCA/EMA integral equations for *arbitrary* $g(r)$ and $V(r)$. The influence of the various parameters has been investigated and a broad comparison of the theory with 'exact' computer simulation data has been carried out for both hard-sphere and Lennard-Jones systems.

We are able to show that the electronic states in the vicinity of the upper band edge are mainly determined by the contact value of $g(r)$, i.e., physically speaking, by nearest-neighbour interactions. This may be understood in terms of an (energy- and density-dependent) screening of the transfer-matrix element [34]. Long-range variations in $g(r)$ do not have any significant influence on the density of states. The correct prediction of the upper band edge may become important when the SSCA/EMA is applied to physical problems where the full band-width of the density of states is needed, (e.g., determining optical absorption phenomena).

When the theoretical results obtained by solving the SSCA/EMA equations numerically are compared with exact molecular dynamics data—the density of states then computed by a direct diagonalization of the Hamiltonian and averaging over uncorrelated configurations—we can summarize our findings as follows.

Due to the neglection of multi-hopping processes in the SSCA/EMA closure we observe only weak agreement at low densities ($\rho^* \leqslant 0.1$). Only the lower band tail agrees well with the simulation, the upper tail deviating noticeably and the upper band edge falling short of the exact value.

At higher densities ($\rho^* \geqslant 0.5$) the theory reproduces the computer simulation quite well, especially at both the band tails. While the position of the upper band edge now almost coincides with the exact position (as does the position of the maximum of the density of states), the peak height of the maximum is overestimated substantially by the theory. This may be attributed—as we show—to the highly selective summation of the diagrams induced by the single-site SSCA/EMA closure, which always tends to overestimate the long-range contributions to the density of states. This behaviour is observed for both hard-sphere and Lennard-Jones systems. This would mean that when one applies this integral-equation approach to problems where the (precise) Fermi energy is required it could become necessary to go beyond the SSCA/EMA single-site approximation.

Finally, the high numerical reliability and accuracy of this implementation has been checked via the calculation of the moments of the density of states, where exact results are known for $\langle E^0 \rangle$, $\langle E^1 \rangle$ up to the second moment $\langle E^2 \rangle$.

Acknowledgments

The authors are indebted to Drs D E Logan and M D Winn (both in Oxford) and to Professor J Hafner (Wien) for many helpful and stimulating discussions. This work was supported by the Österreichische Forschungsfonds under projects P7618-TEC and P8912-PHY. Both authors would like to thank again Dr M D Winn for carefully reading the manuscript.

Appendix

The numerical solution of the coupled integral equations (7), (8) and (11) has been implemented with an appropriate generalization of Gillan's [17] algorithm, well known in the theory of simple liquids, based on a realization of Pastore and Senatore [27]. These equations are solved as described below for a fixed z, increasing z by Δz which was assumed to be at least 0.01. The upper and lower band edges were found by the two criteria $D^*(z) \leqslant 0.001$ and $|D^*(z \pm \Delta z)/D^*(z)| \leqslant 0.01$. As usual one does not solve these equations for the long-ranged $C(x)$ or $H(x)$ (cf. (8) and using reduced units $x = r/d$), but for a complex-valued $\gamma(x) = H(x) - C(x)$ with a discrete representation $\gamma(x_i) = \gamma(i\Delta x), i = 0, \ldots, M$, M being the size of the mesh and Δx its spacing. We have found $\Delta x = 0.05$ and $M = 1025$ data points to give reasonable accuracy while guaranteeing both stable and quick convergence. The number of triangular 'basis-functions' (approximating the 'rough' part of $\gamma(x)$; for convenience we follow the notation of [17]) which is necessary for convergence has been found to depend on the density of the system and the range of the TME. For low-density systems ($\rho^* \leqslant 0.25$) 12–20 basis functions are well suited, whereas in the high-density regime ($\rho^* \geqslant 0.5$) we had to use 20–30 of these functions. It usually suffices to extend these basis functions over 6–8 mesh points. Although one does not normally introduce a mixing parameter for the Picard cycle in Gillan's algorithm,

$$\gamma^{\text{new}}(x) = P(\gamma^{\text{old}}(x)) \tag{A1}$$

(with $P(\gamma)$ denoting the result of applying one Picard iteration to γ) it turned out to be convenient in terms of the convergence rate to do so, especially for higher densities $\rho^* \geqslant 0.5$ and—interestingly—for energy values at the lower band tail:

$$\gamma^{\text{new}}(x) = (1 - \alpha)\gamma^{\text{old}}(x) + \alpha P(\gamma^{\text{old}}(x)). \tag{A2}$$

The iteration for self-consistency is stopped when the convergence criterium

$$\sum_{i=0}^{M} \left|\gamma^{\text{new}}(x_i) - \gamma^{\text{old}}(x_i)\right|^2 \leqslant \epsilon \tag{A3}$$

is fulfilled, $\epsilon = 10^{-8}$ being the value employed in our calculations. When using the SSCA/EMA closure (11) and assuming a mixing parameter $\alpha = 0.1$ convergence was obtained after 1–2 Newton–Raphson cycles, with 1–3 Picard cycles each. Preliminary calculations with a different, multi-hopping closure (22), however, necessitated values of $\alpha \simeq 0.01$ to yield satisfactory convergence behaviour.

From the construction of the Gillan algorithm—it uses Newton's method for minimizing a vector valued complex function—it is evident that one faces an additional difficulty when dealing with HS systems, which possess an intrinsic discontinuity at contact, $g(1^-) \neq g(1^+)$. As the PDF $g(x)$ directly enters our calculations via the closure (11) we have to introduce some form of smoothing at $x = 1$. Of course, without that unphysical smearing, convergence of the algorithm would be utterly impossible. We have chosen an appropriately scaled and shifted $\tanh(\kappa x)$ function, where the slope κ has been determined by requiring good agreement with the known analytical DOS for a V_{Yuk} TME while still guaranteeing self-consistency and convergence of the procedure.

References

[1] Logan D E and Winn M D 1988 *J. Phys. C: Solid State Phys.* **21** 5773
[2] Winn M D and Logan D E 1989 *J. Phys.: Condens. Matter* **1** 1753
[3] Xu B-C and Stratt R 1989 *J. Chem. Phys.* **91** 5613
[4] Wertheim M S 1973 *Mol. Phys.* **25** 211
[5] Hansen J-P and McDonald I R 1986 *Theory of Simple Liquids* 2nd edn (London: Academic)
[6] Kirkwood J G 1935 *J. Chem. Phys.* **3** 300
[7] Roth L M 1974 *J. Physique* **35** C4 317; 1974 *Phys. Rev.* B **9**, 2476; 1975 *Phys. Rev.* B **11** 3769; 1976 *J. Phys. F: Met. Phys.* **6** 2267
[8] Waisman E 1973 *Mol. Phys.* **25** 45
Høye J S, Stell G and Waisman E 1976 *Mol. Phys.* **32** 209
Høye J S and Blum L 1977 *J. Stat. Phys.* **16** 399
[9] Winn M D and Logan D E 1989 *J. Phys.: Condens. Matter* **1** 8683
[10] Bush I J, Logan D E, Madden P A and Winn M D 1989 *J. Phys.: Condens. Matter* **1** 2551; 8735
[11] Xu B-C and Stratt R M 1990 *J. Chem. Phys.* **92** 1923
[12] Chen Z and Stratt R M 1990 *J. Chem. Phys.* **94** 1426; 1992 *J. Chem. Phys.* **97** 5687; 5696
[13] Elyutin P V 1981 *J. Phys. C: Solid State Phys.* **14** 1435
[14] Matsubara T and Toyozawa Y 1961 *Prog. Theor. Phys.* **26** 739
[15] Ishida Y and Yonezawa F 1973 *Prog. Theor. Phys.* **40** 731
[16] Movhagar B and Miller D E 1975 *J. Phys. F: Met. Phys.* **5** 261
[17] Gillan M J 1979 *Mol. Phys.* **38** 1781
[18] Strnadl C F and Kahl G 1993 *J. Non-Cryst. Solids* **156–8** 232
[19] Hansen J-P and Zerah G 1985 *Phys. Lett.* **108A** 277
Zerah G and Hansen J-P 1986 *J. Chem. Phys.* **84** 2336
[20] Allen M P and Tildesley D J 1990 *Computer Simulation of Liquids* (Oxford: Oxford Science)
[21] Arnold A and Mauser N 1990 *Comput. Phys. Commun.* **59** 267
Arnold A, Mauser N and Hafner J 1989 *J. Phys.: Condens. Matter* **1** 965
[22] Wertheim M S 1963 *Phys. Rev. Lett.* **10** 321
Wertheim M S 1964 *J. Math. Phys.* **5** 643
Thiele E 1964 *J. Chem. Phys.* **39** 474
[23] Smith W R and Henderson D 1970 *Mol. Phys.* **19** 411
Kahl G 1989 *Mol. Phys.* **67** 879
[24] Strnadl C F 1993 *Comput. Phys. Commun.* **75** 47
[25] Verlet L and Weis J-J 1972 *Phys. Rev.* A **5** 939
[26] Gibbons M K, Logan D E and Madden P A 1988 *Phys. Rev.* B **38** 7292
[27] Pastore G and Senatore G unpublished
[28] Logan D E private communication
[29] Hafner J, Jaswal S S, Tegze M, Pflugi A, Krieg A, Oelhafen P and Güntherodt H 1988 *J. Phys. F: Met. Phys.* **18** 2583
Jaswal S S and Hafner J 1988 *Phys. Rev.* B **38** 7311
[30] Ganguly K and Stratt R M 1991 *J. Chem. Phys.* **95** 4418; 1992 *J. Chem. Phys.* **97** 1980
[31] Rosenfeld Y and Ashcroft N W 1979 *Phys. Rev.* A **20** 1208
Lado F, Foiles S M and Ashcroft N W 1983 *Phys. Rev.* A **28** 2374
[32] Talbot J, Lebowitz J L, Waismann E M, Levesque D and Weis J-J 1986 *J. Chem. Phys.* **85** 2187

[33] Pastore G and Kahl G 1987 *J. Phys. F: Met. Phys.* **17** L267
Kahl G and Pastore G 1988 *Europhys. Lett.* **7** 37
[34] Logan D E and Wolynes P G 1986 *J. Chem. Phys.* **85** 937
[35] Winn M D and Logan D E 1992 *J. Chem. Phys.* **96** 4818
[36] Barker J A and Henderson D 1967 *J. Chem. Phys.* **47** 4714
[37] Strnadl C F and Kahl G to be published